Achieving ambipolar vertical organic transistors via nanoscale interface modification

Sheng-Han Li, Zheng Xu, Liping Ma, Chih-Wei Chu, and Yang Yang[a]

*Department of Materials Science and Engineering, The Henry Samueli School of Engineering
and Applied Science, University of California, Los Angeles, Los Angeles, California 90095*

Organic field-effect transistors have been the subject of much recent inquiry due to their unique properties. Here, the authors report an ambipolar vertical organic field-effect transistor, which consists of a capacitor cell vertically stacked with an organic active cell, separated by a thin source electrode. By inserting a nanoscale transition-metal-oxide layer at the source/organic interface, the authors fabricated the organic ambipolar transistors with low working voltage and high current output. The thin transition-metal oxide and partial oxidization metal grains form a unique nanostructure that balances the injection barrier height of two types of carriers at the source/organic contact. © 2007 American Institute of Physics. [DOI: 10.1063/1.2773749]

Organic semiconductor devices such as organic light emitting diodes (OLEDs), field-effect transistors, and memory have been studied extensively due to their low-cost, flexible, and large-area application advantages.[1–4] Organic field-effect transistors (OFETs) have high potential as switching devices for active-matrix OLED displays, low-end smart cards and identification tags. However, laterally structured OFETs have two major limitations. (1) device performance, including low current output and high working voltage, and (2) unipolar characteristics, conducting by only one type of carrier. Although in some approaches, for instance, decreasing channel length or increasing the dielectric constant of the gate material are selected to reduce working voltages,[5,6] the transistor output current is still low. Recently, we reported a vertical organic field-effect transistor (VOFET),[7] with low working voltage and high current output. This device structure should provide an opportunity to solve the low current output problem.

Most OFETs show either *N* or *P* channel behavior (conduct by holes or electrons inside the transistor channel). In integrated circuits, especially complementary metal-oxide semiconductor (CMOS) circuits, the system needs both *N*- and *P*-type transistors to function. The use of ambipolar OFETs could simplify the CMOS design and fabrication processes. Ambipolar OFETs have been fabricated by applying blends,[8] bilayers of carrier transporting materials,[9] and electron injection electrodes.[10] However, the operating voltage for these technologies is still not low enough for some applications.

In this letter, we demonstrate an ambipolar VOFET by inserting a transition-metal-oxide layer at the source/organic interface to form a unique nanoscale structure. Within this charge injection layer, the transistor shows high output current for both *N*-type and *P*-type operational modes. The device structure [Fig. 1(a)] consists of an active cell stacked with a capacitor cell. The thin middle electrode is defined as the common-source electrode. The top electrode and the bottom electrode are defined as the drain and gate electrode, respectively. A charge injection layer is inserted between the contact of the organic layer and the electrodes. Figure 1(b)

shows the operating modes for an ambipolar VOFET. During the operation the source electrode is always grounded. By applying different polarities of voltage bias to the gate and the drain electrodes, the ambipolar behavior can be observed: a negative bias results *P*-type [Fig. 1(b), left side] conduction while a positive bias results *N*-type conduction [Fig. 1(c), right side].

The ambipolar transistor, fabricated via thermal evaporation according to the structure of Fig. 1(a), consists of, from the bottom up, glass/Aluminum (Al) (35 nm)/Lithium fluoride (LiF) (150 nm)/Al (20 nm)/Vanadium pentoxide (V_2O_5) (7.5 nm)/Pentacene (120 nm)/V_2O_5 (7.5 nm)/ Al(35 nm). The pressure during deposition was better than 4×10^{-6} torr. Pentacene and V_2O_5 were purchased from Aldrich and were used as received. The device area is 2.4 mm^2, defined by the crossover area between the drain and source electrodes. In this letter, all devices were examined with an ambient relative humidity of 45% using an Agilent 4155C precision semiconductor parameter analyzer.

The energy alignment at source organic interfaces was measured by an Omicron NanoTechnology system with He I excitation (21.2 eV) for ultraviolet photoelectron spectroscopy (UPS) spectra. LiF (30 nm) was deposited onto a pre-
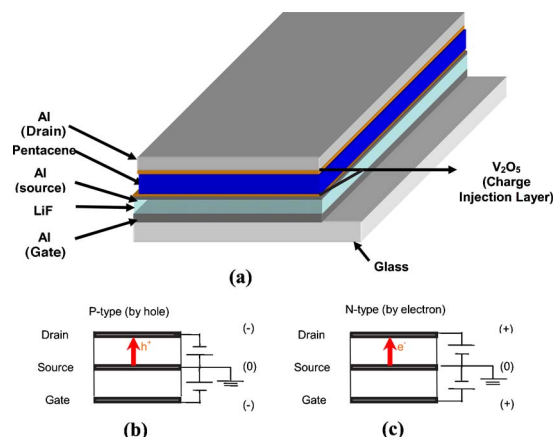
FIG. 1. (Color online) (a) Schematic cross-sectional diagram of the proposed ambipolar VOFET structure. (b) Ambipolar device operating modes for *P* type. (c) Ambipolar device operating modes for *N* type.

[a]Electronic mail: yangy@ucla.edu
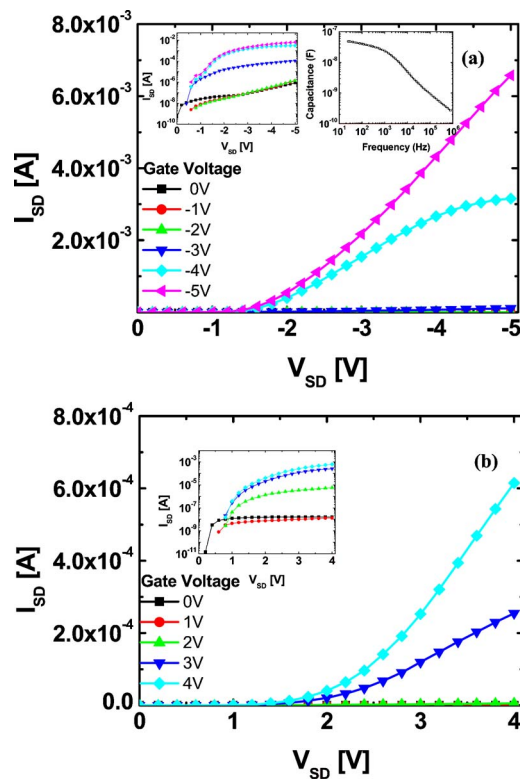
FIG. 2. (Color online) (a) VOFET with V_2O_5 as the carrier injection layer resulting in *P*-type operation. The gate voltage is varied from 0 to -5 V with 1 V steps. The inset figures depict a logarithmic scale used to extract the device on/off ratio (left) and the capacitance of the bottom capacitor cell (right). (b) Transistor behavior for *N*-type operation.

cleaned indium tin oxide glass substrate. Al (20 nm) followed as simulated source electrode layer, and then the charge injection layer, vanadium pentoxide (15 nm), took place. After the deposition, the sample was immediately transferred to the prepare chamber of an Omicron XPS/UPS system. A thin pentacene layer, 5 nm, was deposited on top of the sample surface under ultrahigh vacuum. The samples were transported into the analysis chamber for XPS/UPS measurement. The base pressure of the XPS/UPS system is better than 10^{-9} mbar. UPS spectra were recorded with a sample bias of -5 V.

In Figs. 2(a) and 2(b), source-drain currents (I_{SD}) versus source-drain voltages (V_{SD}) are plotted for *P*- and *N*-type behaviors under different operating conditions. When operated as a *P*-type device, the output current was 6.6 mA, with on/off ratio up to 10^4 [V_{SD} and gate voltage (V_G) both at negative 5 V]. When operated as a *N*-type device, transistor showed an output current around 0.610 mA with on/off ratio larger than 10^4. The inset figure depicts the capacitance of the capacitor cell, which is consistent with our previous results.[7] The gate leakage currents, the current from the gate electrode to the source electrode at negative or positive 5 V gate bias, were both under 5 μA. Devices without V_2O_5 layer only show *N*-type behavior only. Comparing device *P*-type behaviors, we should expect that adding a V_2O_5 layer plays an important role in the *P*-type operating mechanism.

A thin, rough surface, and nanoscale partial oxidization metal grains is the requirement for fabricating an ambipolar VOFET source electrode. A thin source electrode cross-sectional transmission electron microscope (TEM) image [Fig. 3(a)] indicates that source metal line is not composed of
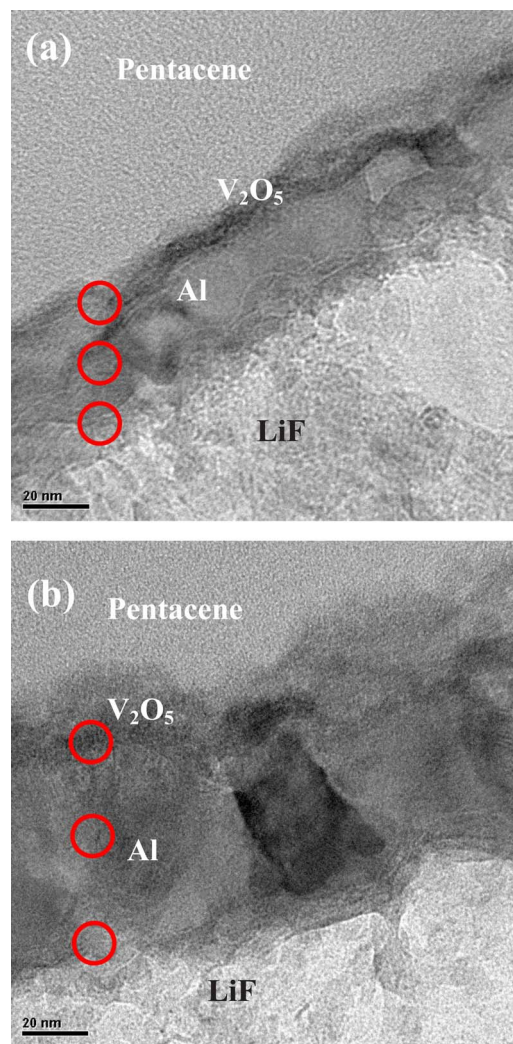
FIG. 3. (Color online) Cross-sectional TEM image of (a) the thin source electrode (20 nm) and (b) the thick source electrode (60 nm). Note the granular structure of Al within the film. The red marks indicate the locations where the EDX analysis was performed. For (a), all three locations show V signal. For (b), only the top circle shows V signal.

a flat and continuous Al film. Actually, the film is composed of discontinuous Al grains which are surrounded by aluminum oxide and V_2O_5 nanodomains. The discontinuous nature of the Al film may allow the organic film to contact the dielectric layer directly. Due to these thin oxide layers, the electric field induced by the gate bias might penetrate through the discrete electrode of the Al grains.[11] Moreover, energy dispersive x-ray (EDX) analysis also illustrates that the source electrode is a combination of Al, alumina, and V_2O_5.[12] The thick source electrode (60 nm) cross-sectional TEM image [Fig. 2(b)] shows a different morphology, compared with thin electrode image. The V_2O_5 layer only covers the top of the Al electrode. From EDX data, we can observe that the vanadium signals vanished at the center and the bottom of the thick electrode, which means that all the possible cracks and pinholes inside the source electrode are filled by the growing Al grains. Those enlarged grains block the influence of the gate bias, because of the free electron in metal grains. This might be a reasonable explanation since the modification behavior finally vanishes after a certain source electrode thickness.

A proper charge injection barrier between the source electrode and the organic layer is the second requirement for
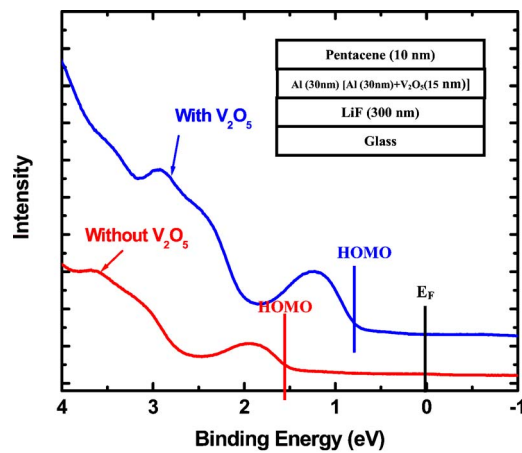
FIG. 4. (Color online) XPS valence band spectra acquired with He I (21.2 eV) on samples with (blue line) and without V_2O_5 (red line). The HOMO position is determined by the intersection of the onset of the peak at the lowest binding energy and the background. Fermi level is located at zero binding energy. The inset shows the sample structures.

the VOFET operation. In order to understand the energy level alignments at the interface, we applied UPS to investigate the V_2O_5/pentacene system. Details of the procedure for determining the energy level alignment of such interfaces using UPS are described elsewhere.[13–17] In our previous work, we used XPS/UPS to investigate the working mechanism of vertical transistors.[11] Here, the electron and hole injection barriers were studied using UPS. The samples for UPS testing were fabricated in the same evaporator where our devices were made except pentacene which was deposited under ultrahigh vacuum. The valence band of pentacene and the sample structure are shown as Fig. 4 and its inset, respectively. The zero point of the binding energy is set as the Fermi edge determined from Ag. The highest occupied molecular orbital (HOMO) position is determined by the intersection of the onset of the peak at the lowest binding energy and the background. For the sample without V_2O_5 (red line), the HOMO of pentacene is located at 1.4 eV below the Fermi level. Accordingly, the hole injection barrier between Al electrode and pentacene (about 1.4 eV) is much higher than the electron injection barrier (0.4 eV, here assuming the optical band gap equals the difference between the lowest energy molecular orbital and HOMO). The large hole injection barrier explains that transistors with Al source electrode only show *N*-type behavior. The upper spectrum (blue line) of Fig. 4 was obtained from the sample with 15 nm V_2O_5. The HOMO is located at about 0.7 eV below the Fermi level which corresponds to a low hole injection barrier ($\sim$0.7 eV) and a high electron injection barrier (1.1 eV). The energy level alignment has been adjusted by adding a thin layer of V_2O_5. Our previous work, using Al/V_2O_5 stacking electrode for lateral pentacene transistors, also shows the improvement of hole injection.[18] When the V_2O_5 layer is discontinuous, holes can be injected at covered parts of the interface. Meanwhile, electrons can be injected at those uncovered parts. In order to achieve the ambipolar transistor, the nanoscale mixture of partial-oxidized Al and V_2O_5 grains is essential. The ambipolar device operation mechanism can be described in the following manner. The I_{SD} should be

controlled by carrier injection from the source electrode into the organic film. At zero gate bias, the injection barrier is high enough to confine the carriers injected from source to organic, so I_{SD} is quite low at zero gate bias. When the gate is under positive or negative bias, the capacitor is fully charged with buildup charges. Due to the rough and partially oxidized interface, those charges may align the water molecules or the ions dissolved in the water to create interface dipoles at the interface between electrode and organic film. The dipoles created by buildup charges can be modulated by the gate bias. As a result, the injection barrier height is likewise modified and decreases with increasing gate bias. The formation and role of the interface dipoles will be described in more detail in a separate paper.[12]

In summary, we have studied the ambipolar properties of vertical organic field-effect transistors; V_2O_5 and partial-oxidized Al were utilized to form a nanoscale composite source electrode. The particular significant role of the transition-metal oxide is lowering the hole injection barrier at the organic interface. The electron injection barrier is still controlled by Al and pentacene contact or the tunneling current from source to organic layer. With this ambipolar behavior, the illustrated device may open an application direction for organic field-effect transistors.

[1] C. W. Tang and S. A. VanSlyke, Appl. Phys. Lett. **51**, 913 (1987).
[2] J. H. Burroughes, D. D. C. Bradley, A. R. Brown, R. N. Marks, K. Mackay, R. H. Friend, P. L. Burns, and A. B. Holmes, Nature (London) **347**, 539 (1990).
[3] G. Horowitz, Adv. Mater. (Weinheim, Ger.) **10**, 365 (1998).
[4] L. P. Ma, J. Liu, and Y. Yang, Appl. Phys. Lett. **80**, 2997 (2002).
[5] C. D. Dimitrakopoulos, S. Purushothaman, J. Kymissis, A. Callegari, and J. M. Shaw, Science **283**, 822 (1999).
[6] M. J. Panzer, C. R. Newman, and C. D. Frisbie, Appl. Phys. Lett. **86**, 103503 (2005).
[7] L. P. Ma and Y. Yang, Appl. Phys. Lett. **85**, 5084 (2004).
[8] E. J. Meijer, D. M. De Leeuw, S. Setayesh, E. Van Veenendaal, B.-H. Huisman, P. W. M. Blom, J. C. Hummelen, U. Scherf, and T. M. Klapwijk, Nat. Mater. **2**, 678 (2003).
[9] A. Dodabalapur, H. E. Katz, L. Torsi, and R. C. Haddon, Appl. Phys. Lett. **68**, 1108 (1996).
[10] T. Yasuda, T. Goto, K. Fujita, and T. Tsutsui, Appl. Phys. Lett. **85**, 2098 (2004).
[11] Z. Xu, S. H. Li, and Y. Yang (unpublished).
[12] S. H. Li, Z. Xu, and Y. Yang (unpublished).
[13] L. Yan, M. G. Mason, C. W. Tang, and Y. L. Gao, Appl. Surf. Sci. **175-176**, 412 (2001).
[14] P. G. Schroeder, C. B. France, J. B. Park, and B. A. Parkinsona, J. Appl. Phys. **91**, 3010 (2002).
[15] R. J. Murdey and W. R. Salaneck, Jpn. J. Appl. Phys., Part 1 **44**, 3751 (2005).
[16] X. Crispin, V. Geskin, A. Crispin, J. Cornil, R. Lazzaroni, W. R. Salaneck, and J. L. Brédas, J. Am. Chem. Soc. **124**, 8131 (2002).
[17] R. H. Friend, R. W. Gymer, A. B. Holmes, J. H. Burroughes, R. N. Marks, C. Taliani, D. D. C. Bradley, D. A. Dos Santos, J. L. Brédas, M. Lögdlund, and W. R. Salaneck, Nature (London) **397**, 121 (1999).
[18] C. W. Chu, S. H. Li, C. W. Chen, V. Shrotriya, and Y. Yang, Appl. Phys. Lett. **87**, 193508 (2005).